Frequency Conversion Using a Moving Plasma Front Generated Optically in Transmission Lines – Theoretical Analyses –

Jongsuck Bae and Koji Mizuno

Research Institute of Electrical Communication, Tohoku University, 2-1-1 Katahira, Aoba-ku, Sendai 980-8577, Japan

Abstract — **A novel method for frequency conversion using a transmission line on a semiconductor substrate has been presented. Laser pulses move along the transmission line as generating an electron-hole plasma at the surface of the semiconductor substrate. The plasma in the transmission line acts as a moving short with a relativistic velocity, reflecting an incident microwave and up-shifting the frequency through the double Doppler effect. Power and energy conversion efficiencies have been theoretically analyzed for the frequency conversion. The results have shown that the converter can be used to produce short millimeter and submillimeter waves.**

I. Introduction

Frequency conversion with the Doppler shift is one of ideal methods to generate high frequency electromagnetic waves with high power, because it can achieve high frequency conversion ratios with high efficiency in an extremely wide frequency range. For this type of frequency conversion, some reflectors which move at a relativistic speed are required. Since it is difficult in practice to realize such reflectors, its applications have been strongly limited to high-energy electron beam devices such as free electron lasers.

In this paper, a novel method of frequency conversion using an optically generated plasma in semiconductors as a moving reflector is presented.

II. Configuration of the Frequency Converter

Figure 1 shows the schematic diagram of the frequency converter proposed in this paper. This converter consists of an optical delay line, a transmission line with a semiconductor substrate, and a frequency filter. The transmission line is supposed to be one of microwave transmission lines including coplanar waveguides, slot lines, and fined or ridged waveguides. We will call it TLFC (transmission line type frequency converter) for short.

In the TLFC, laser pulses travel along a transmission line as generating an electron-hole plasma at the surface of the semiconductor substrate. Since the process of optical excitation of free carriers in semiconductors is

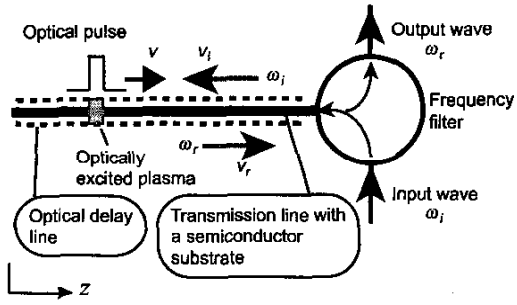

Fig. 1 Schematic drawing of the frequency upconverter using an optically generated plasma in a semiconductor substrate of a transmission line.

extremely fast, the plasma boundary moves with the laser pulse at a velocity v without a notable delay. The moving plasma boundary reflects an incident wave, shifting its frequency ω_i into a higher one ω_r through the double Doppler effect. The frequency ratio F_g is given by

$$F_g = \omega_r / \omega_i = (1+\beta_i)/(1-\beta_r) \qquad (1)$$

where $\beta_i = v/v_i$, $\beta_r = v/v_r$, and v_i and v_r are the phase velocities of the incident and reflected waves, respectively. Since v and v_r can be adjusted by choosing the line configurations, high F_g over 10 are easily achievable.

In the TLFC, the optically generated plasma itself is stationary and only its boundary moves. Lampe et al. theoretically analyzed wave reflection at a moving boundary of a stationary plasma in an isotropic medium (free space) [1]. The Lamp's theory has been applied for the TLFC to assess its feasibility. The results have shown that the frequency of the reflected wave is up-shifted at the ratio given by Eq. (1), but its amplitude is not amplified. An energy conversion efficiency η_W in the TLFC thus is decreased by $1/F_g$ due to time compression for a duration of the reflected pulse. This is different from the case of actually moving plasma in which η_W increases by F_g times.

The energy loss in TLFCs, however, does not depend on the operation frequencies, thus η_W=10 % for F_g= 10 can be achieved even at submillimeter wave frequencies

0-7803-7695-1/03/$17.00 © 2003 IEEE

in principle. In addition, TLFCs are highly tunable because any resonator is not required for frequency conversion.

III. THEORY

A. Propagation constants

To simplify the analysis, the following assumptions have been made for the transmission line; (a) a TEM_{00}-mode transmission, (b) dispersionless, (c) no propagation loss except for rf-loss associated with an optically generated plasma, (d) a constant shunt conductance per a unit length, G, with the plasma, and (e) an abrupt plasma boundary compared to the wavelengths of all electromagnetic waves in the transmission line.

Referring to Fig. 1, the plasma (reflection) front moves at a relativistic velocity in the $+z$-direction. Therefore, a conduction current in the plasma is left behind the reflection front, causing rf-loss. In order to take the loss into account, the analysis has been curried out in the moving reflection front frame (the "front frame").

The differential equations for the transmission line in the front frame is given by

$$\frac{\partial V}{\partial z}=\frac{\partial \Phi}{\partial t},\quad \frac{\partial I}{\partial z}=I_G+\frac{\partial Q}{\partial t} \tag{2}$$

where V is a voltage, I is a current, I_G is the conduction current in the plasma, Φ and Q are the magnetic flux and the electric charge for a unit length, respectively.

In the front frame, the transmission line including the semiconductor substrate moves at the velocity v in the $-z$-direction, and only the boundary is stationary. Therefore, I_G changes depending on position, z, as well as time, t, so that the differential equation for I_G is given by

$$\frac{\partial I_G}{\partial t}-v\frac{\partial I_G}{\partial z}=j\omega G(V-v\Phi) \tag{3}$$

In the laboratory frame, $\Phi^*=L^*I^*$ and $Q^*=C^*V^*$ are valid, but in the front frame, $\Phi\neq LI$ and $Q\neq CV$ due to an anisotropy in the moving transmission line [2], where L is the inductance per a unit length and C is the capacitance per a unit length, and asterisks denote quantities in the laboratory frame. The relations between Φ and I, Q and V in the moving transmission line are as follows;

$$\Phi-\frac{v}{c^2}V=L^*(I-vQ),\quad Q-\frac{v}{c^2}I=C^*(V-v\Phi) \tag{4}$$

where c is the velocity of electromagnetic waves in free space. From Eq. (4), we obtain the following relations,

$$\Phi=\gamma_p^2\left\{\gamma^{-2}L^*I-v\left(\frac{1}{v_p^2}-\frac{1}{c^2}\right)V\right\} \tag{5}$$

$$Q=\gamma_p^2\left\{\gamma^{-2}C^*V-v\left(\frac{1}{v_p^2}-\frac{1}{c^2}\right)I\right\} \tag{6}$$

where

$$v_p=1/\sqrt{L^*C^*},\quad \gamma=1/\sqrt{1-\beta^2},\quad \gamma_p=1/\sqrt{1-\beta_p^2},$$
$$\beta=v/c,\quad \beta_p=v/v_p$$

Assuming spatial and temporal dependence, $\exp(j\omega t+kz)$, Eqs. (2)-(6) lead to the dispersion relation

$$(1-\frac{k}{\omega}v)\left\{\left[k+\frac{\omega}{v_p}\gamma_p^2\left(\beta_p-\frac{\beta^2}{\beta_p}\right)\right]^2-\frac{\omega^2}{v_p^2}\frac{\gamma_p^4}{\gamma^4}\left[1-j\frac{G}{\omega C^*}\frac{\gamma^2}{\gamma_p^2}\right]\right\}=0 \tag{7}$$

Solving this equation, we obtain three waves,

$$k_G=\omega/v \tag{8}$$

$$k^{\pm}=\frac{\omega}{v_p}\gamma_p^2\left[\frac{\beta^2}{\beta_p}-\beta_p\pm\frac{A(G)}{\gamma^2}\right] \tag{9}$$

$$\text{where } A(G)=\sqrt{1-j\frac{G}{\omega C^*}\frac{\gamma^2}{\gamma_p^2}}$$

The first wave component, $(V_G, I_G)\exp[j(\omega t+k_Gz)]$, in the front frame is Lorentz-transformed to $(V_G^*=0,\ I_G^*=I_G/\gamma)\exp(jk_G^*z^*)$ in the laboratory frame. I_G^* is the current left in the plasma region and is consumed as heat in the plasma.

In Eq. (9), k^+ and k^- are the propagation constants for the waves of travel in the $-z$ and $+z$ directions, respectively. These propagation constants are consistent with Lampe's ones for $v_p=c$. When $v=0$, k^+ and k^- agree with propagation constants in conventional transmission lines. It should be noted that $A(G)$ is rewritten and is approximately given by

$$A(G)\approx\sqrt{1-j\frac{G^*}{\omega_r^*C^*}} \tag{10}$$

where G^* is the shunt conductance in the laboratory frame. Eq. (10) indicates that the loss term is determined by the output frequency ω_r^* of the reflected wave.

B. Conversion efficiencies

The amplitudes of the waves shown in Fig. 2 have been determined by using the boundary conditions,

$$V_i+V_r=V_t+V_G \tag{11-a}$$

$$I_i - I_r = I_t + I_G \qquad (11\text{-b})$$

$$\frac{\partial I_i}{\partial z} - \frac{\partial I_r}{\partial z} = \frac{\partial I_t}{\partial z} + \frac{\partial I_G}{\partial z} \qquad (11\text{-c})$$

The third condition has been introduced to determine three unknown amplitudes, i.e., V_r, V_t, and V_G. In Eqs. (11), the relations between V and I, V and $\partial I/\partial z$ are given by $V=ZI$ and $\partial I/\partial z=jkV/Z$, where the characteristic impedances Z are

$$Z_1 = Z_0 = \sqrt{L^* / C^*}\ ,\ Z_2 = Z_0 / A(G)\ ,\ Z_G = vL^*$$

The solutions of Eqs. (11) for the reflectance Γ is

$$\Gamma = \frac{V_r}{V_i} = \frac{1-\beta_p}{1+\beta_p}\frac{Z_2 - Z_1}{Z_2 + Z_1} \qquad (12)$$

The power reflectance is also given by

$$\frac{P_r}{P_i} = \left(\frac{1-\beta_p}{1+\beta_p}\right)^2 |\Gamma_0|^2 \qquad (13)$$

where $\Gamma_0=(Z_2-Z_1)/(Z_2+Z_1)$ which is almost the same as the reflectance for a stationary sharp plasma front when the plasma density is high enough to be $G \gg \omega C^* \gamma_p^2/\gamma^2$, and thus $\Gamma_0 \sim -1$.

The expressions of Eqs. (12) and (13) are the same as Lampe's ones, except for a change of β for β_p. Therefore, the discussion on the power and energy conversion efficiencies in the laboratory frame is the same as Lampe's ones. We write down these expressions;

$$F_g = \omega_r^* / \omega_i^* = \tau_i^* / \tau_r^* = (1+\beta_p)/(1-\beta_p) \qquad (14)$$

$$\eta_W^* \equiv \frac{W_r^*}{W_i^*} = \frac{\omega_r^*}{\omega_i^*}\frac{W_r}{W_i} = \frac{|\Gamma_0|^2}{F_g} \qquad (15)$$

$$\eta_P^* \equiv \frac{P_r^*}{P_i^*} = \frac{W_r^*}{W_i^*}\frac{\tau_i^*}{\tau_r^*} = |\Gamma_0|^2 \qquad (16)$$

where τ_i^* and τ_r^* are the durations of the incident and reflected pulses, respectively, W stands for energy and P for power, η_W^* is the energy conversion efficiency and η_P^* is the power conversion efficiency.

As seen from Eq. (15), the frequency conversion in TLFCs involves energy loss due to the reduction of the time duration of the reflected pulse. It should be noted that the energy loss depends not on the operation frequencies themselves, but on the frequency conversion ratio, F_g.

C. Wave matrix

For calculation of η_P^* in TLFCs with multiple

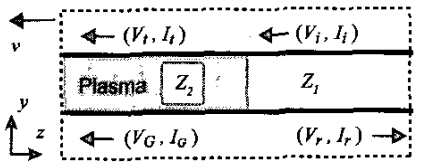

Fig. 2 Waves at the plasma boundary. Z_1 and Z_2 are the characteristic impedances of the transmission lines with and without the plasma, respectively.

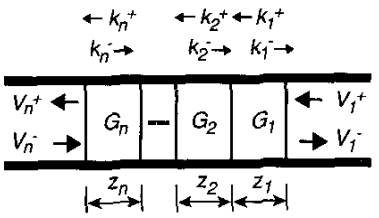

Fig. 3 Waves in the multiple boundaries.

boundaries, a wave matrix has been derived. Referring to Fig. 3,

$$\begin{bmatrix} V_1^+ \\ V_1^- \end{bmatrix} = M_{1a} M_{1b} M_{2a} M_{2b} \cdots\cdots M_{na} \begin{bmatrix} V_n^+ \\ V_n^- \end{bmatrix} \qquad (17\text{-a})$$

$$M_{ma} = \begin{bmatrix} \dfrac{1-\beta_p A_m}{1-\beta_p A_{m-1}}\dfrac{Z_m + Z_{m-1}}{2Z_m} & \dfrac{1+\beta_p A_m}{1-\beta_p A_{m-1}}\dfrac{Z_m - Z_{m-1}}{2Z_m} \\ \dfrac{1-\beta_p A_m}{1+\beta_p A_{m-1}}\dfrac{Z_m - Z_{m-1}}{2Z_m} & \dfrac{1+\beta_p A_m}{1+\beta_p A_{m-1}}\dfrac{Z_m + Z_{m-1}}{2Z_m} \end{bmatrix} \qquad (17\text{-b})$$

$$M_{mb} = \begin{bmatrix} e^{ik_m^+ z_m} & 0 \\ 0 & e^{ik_m^- z_m} \end{bmatrix} \quad for\ m = 1, 2, \ldots, n \qquad (17\text{-c})$$

where $A_m=A(G_m)$ and $Z_m=Z_0/A_m$.

The wave matrix in Eqs. (17) is similar to the one calculated by Tsai *et al.* for multiple boundaries of dielectric media in the laboratory frame [3], but in our case the conductive media in the front frame.

IV. Simulation Results

Figure 4 shows one of possible TLFC configurations. For this converter, the power conversion efficiencies η_P^* have been calculated using the formulas derived in Sec. III. The simulation has focused on the dependence of η_P^* on the shunt conductance G and its spatial distribution at the boundary, so that a propagation loss and a frequency dispersion in the coplanar waveguide have been ignored. In the calculation, the following parameters were used;

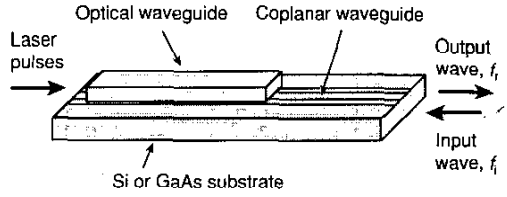

Fig. 4 A possible TLFC configuration using a coplanar waveguide.

for the coplanar waveguide;
Z_0= 50 Ω, v_p=c/2.57, C^*(=1/Z_0v_p)=171 pF/m, and the gap d_g=35 μm between the metal lines
for the laser beam;
the wavelength = 532 nm, a penetration depth d_p=2.4 μm (in Si)

In the calculation, the spatial distribution $N(z)$ of the plasma density at the boundary was given by assuming excitation with a Gaussian laser pulse,

$$N(z) = n_p^* erf(\sqrt{2}z / vt_p^*)$$

where n_p^* is the maximum carrier density and t_p^* is the laser pulse width in the laboratory frame. The shunt conductance $G(z)$ has been determined for the plasma density $N(z)$ using the relation, $G(z)=eN(z)$ $(\mu_e+\mu_h)d_p/d_g$, where e is the electron charge, μ_e and μ_h are the mobility of electron and hole, respectively. In the simulation, the plasma boundary having the spatial distribution $N(z)$ has been treated as a series of abrupt interfaces between short transmission lines where G are constant. η_P^* was calculated using the wave matrix in Eq. (17).

The simulation results for F_g=10 (v=c/3.14) are shown in Figs. 5 and 6. As seen from the results, η_P^* changes strongly depending on n_p^* and t_p^*. For n_p^* =10^{21}/cm^3 and t_p^* = 2 psec, η_P^*=0.8 at f_r=1 THz. The energy conversion efficiency thus is 8 %. The plasma density of 10^{21}/cm^3 corresponds to a laser energy of 1 mJ for an interaction length of 1 cm between the plasma and the incident wave.

Similar calculations have been done for different F_g of 20 and 30 in the same output frequency range. The calculated results have been almost the same as the ones shown in Figs. 5 and 6 for F_g =10, as described for Eq. (10). It is a significant feature of the TLFC.

V. Conclusion

The Doppler shifts of microwaves reflected from a moving plasma boundary generated optically in a transmission line has been analyzed theoretically. The results have suggested that this method for frequency conversion could be used to generate short millimeter and submillimeter waves with a high efficiency.

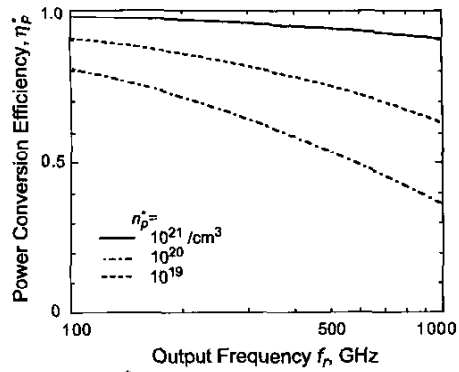

Fig. 5 Calculated η_P^* vs. the reflected frequency f_r for F_g =10 and t_p^* = 2 psec.

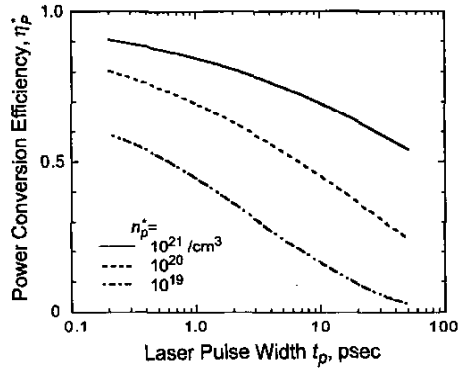

Fig. 6 Calculated η_P^* vs. the laser pulse width t_p^* for F_g =10 at f_r=1 THz.

References

[1] M. Lampe, D. Ott, J. H. Walker, "Interaction of electromagnetic waves with a moving ionization front," *Phys. Fluds*, vol. 21, no. 1, pp. 42-54, Jan. 1978.
[2] R. C. Costen and D. Adamson, "Three-Dimensional Derivation of the Electrodynamic Jump Conditions and Momentum-Energy Laws at a Moving Boundary," *Proc. IEEE*, vol. 53, no. 9, pp. 1181-1196, Sept. 1965.
[3] C. S. Tsai and B. A. Auld, "Wave Interaction with Moving Boundaries," *J. Appl. Phys.*, vol. 38, no. 5, pp. 2106-2115, April 1967.